An EXAFS Study of the Interaction of Substrate with the Ferric Active Site of Protocatechuate 3,4-Dioxygenase†

Anne E. True,‡ Allen M. Orville,§ Linda L. Pearce,‡ John D. Lipscomb,§ and Lawrence Que, Jr.*,‡
Departments of Chemistry and Biochemistry, University of Minnesota, Minneapolis, Minnesota 55455
Received May 31, 1990; Revised Manuscript Received August 24, 1990

ABSTRACT: X-ray crystallographic studies of the intradiol cleaving protocatechuate 3,4-dioxygenase from *Pseudomonas aeruginosa* have shown that the enzyme has a trigonal bipyramidal ferric active site with two histidines, two tyrosines, and a solvent molecule as ligands [Ohlendorf, D. H., Lipscomb, J. D., & Weber, P. C. (1988) *Nature 336*, 403–405]. Fe K-edge EXAFS studies of the spectroscopically similar protocatechuate 3,4-dioxygenase from *Brevibacterium fuscum* are consistent with a pentacoordinate geometry of the iron active site with 3 O/N ligands at 1.90 Å and 2 O/N ligands at 2.08 Å. The 2.08-Å bonds are assigned to the two histidines, while the 1.90-Å bonds are associated with the two tyrosines and the coordinated solvent. The short Fe–O distance for the solvent suggests that it coordinates as hydroxide rather than water. When the inhibitor terephthalate is bound to the enzyme, the XANES data indicate that the ferric site becomes 6-coordinate and the EXAFS data show a beat pattern which can only be simulated with an additional Fe–O/N interaction at 2.46 Å. Together, the data suggest that the oxygens of the carboxylate group in terephthalate displace the hydroxide and chelate to the ferric site but in an asymmetric fashion. In contrast, protocatechuate 3,4-dioxygenase remains 5-coordinate upon the addition of the slow substrate homoprotocatechuic acid (HPCA). Previous EPR data have indicated that HPCA forms an iron chelate via the two hydroxyl functions. For the iron site to remain 5-coordinate and the HPCA to be chelated to the iron, the substrate must displace not only the hydroxide but also a ligand from the protein backbone, probably a histidine. The mechanistic implications of the displacement of hydroxide and a protein ligand in the active site are discussed.

Protocatechuate 3,4-dioxygenase (3,4-PCD) catalyzes the cleavage of protocatechuate (3,4-dihydroxybenzoate) to β-carboxy-*cis*,*cis*-muconic acid with incorporation of the elements of dioxygen [Fujisawa & Hayaishi, 1968; for a review, see Que (1989)]. This non-heme iron containing enzyme mediates the critical ring opening step in the pathways of biodegradation of many aromatic compounds, and it has been reported to be present in at least 10 bacterial strains spanning the aerobic genera (Durham et al., 1980). Along with catechol 1,2-dioxygenase, 3,4-PCD serves as the prototypical protein for the class of iron–tyrosinate proteins (Que, 1983) that are characterized by a distinctive visible absorption spectrum arising from tyrosinate-to-iron(III) charge-transfer transitions; this assignment has been confirmed by resonance Raman spectroscopy (Felton et al., 1978; Keyes et al., 1978; Que & Epstein, 1981). Spectroscopically and mechanistically, all of the well-studied 3,4-PCD's are very similar. The enzyme isolated from *Brevibacterium fuscum* has been utilized for many spectroscopic investigations because the environment of the iron is apparently very homogeneous and exhibits well-resolved spectra (Whittaker et al., 1984). The 3,4-PCD from *Pseudomonas aeruginosa* has been characterized crystallographically to a resolution of 2.8 Å as a dodecamer of two nonidentical subunits, i.e., $(\alpha\beta Fe^{3+})_{12}$ (Ohlendorf et al., 1988). The 3,4-PCD's isolated from other strains all have the same fundamental $\alpha\beta Fe^{3+}$ structure, but the number of dimeric units varies (Durham et al., 1980). The active site of the *P. aeruginosa* enzyme lies at the interface between the α and β subunits with the catalytic ferric ion coordinated by four residues from the β subunit: Tyr 118, Tyr 147, His 160, and His 162. The iron coordination geometry forms an approximate trigonal bipyramid with Tyr 147(β) and His 162(β) located in the axial positions as shown:

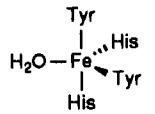

The third coordination site in the equatorial plane has electron density that has been attributed to a bound solvent molecule. The crystallographic results corroborate the active site model (Pyrz et al., 1985) proposed on the basis of spectroscopic studies (Que et al., 1976; Felton et al., 1978: Que & Epstein, 1981; Felton et al. 1982; Roe et al., 1984; Whittaker & Lipscomb, 1984). While the X-ray diffraction study has established gross details of the active site coordination environment of the native enzyme, its 2.8-Å resolution is insufficient to resolve the more precise aspects of metal–ligand bond lengths. Furthermore, important questions regarding the impact of changes in the iron coordination environment during catalysis cannot be directly addressed from the crystal structure of the native enzyme.

As the iron appears not to be reduced during the catalytic cycle (Que et al., 1976; Bull et al., 1981; Walsh et al., 1983; Whittaker & Lipscomb, 1984), a novel substrate activation mechanism has been proposed for 3,4-PCD (Que et al., 1977; Whittaker & Lipscomb, 1984; Cox & Que, 1988). In this mechanism the catecholic substrate is activated by chelation of the ferric ion and dioxygen directly attacks the aromatic ring. Evidence for substrate chelation has been educed from both NMR (Lauffer & Que, 1982) and EPR (Orville & Lipscomb, 1989) studies. It is likely that one of the substrate hydroxyl groups coordinates to the iron by displacing the solvent molecule bound to the active site iron (Whittaker &

† This research was supported by National Institutes of Health Grants GM-33162 (L.Q.) and GM-24689 (J.D.L.). A.E.T. is grateful for a National Research Service Fellowship from the NIH (GM-12792).
‡ Department of Chemistry.
§ Department of Biochemistry.

0006-2960/90/0429-10847$02.50/0

Lipscomb, 1984; Orville & Lipscomb, 1989). However, it is not known whether the second substrate hydroxyl is accommodated by expansion of the iron coordination number or by displacement of one of the protein ligands to the iron.

Metric details of the active site environment of the iron center can, in principle, be obtained by using X-ray absorption spectroscopy (Scott, 1985). The previously reported EXAFS study of 3,4-PCD from *P. aeruginosa* did not address this question, presumably due to insufficient signal to noise in the data (Felton et al., 1982). In this study, we take advantage of the more homogeneous active site of the 3,4-PCD from *B. fuscum* to afford insights into the coordination environment of the iron in the native enzyme and the changes engendered by the binding of the inhibitor terephthalate and the slow substrate homoprotocatechuate (HPCA).

Experimental Procedures

Preparation of Protein Samples. 3,4-PCD was isolated from *B. fuscum* (ATCC 15993) as previously described (Whittaker et al., 1984, 1990). The EXAFS sample for native 3,4-PCD had a concentration of 1 mM protein (5 mM iron) in 50 mM MOPS buffer at pH 7.0. Iron concentrations were determined by using inductively coupled plasma emission spectroscopy and A_{434} measurements (ϵ_{434} = 2.9 mM^{-1} cm^{-1}/Fe) (Whittaker et al., 1984). Neutralized 0.5 M stock solutions of terephthalate and HPCA from Aldrich were made in 0.1 M MOPS buffer at pH 7.0. The terephthalate complex was prepared by the aerobic addition of the inhibitor to 1 mM 3,4-PCD to give a final terephthalate and iron concentration of 23 and 4.3 mM, respectively. For the anaerobic substrate complex, the protein was degassed and cycled with argon passed over a BASF copper catalyst at 170 °C to remove trace oxygen. Anaerobic HPCA was added to the anaerobic enzyme to generate a sample with 35 mM HPCA and a final iron concentration of 4.3 mM.

EXAFS Data Collection and Analysis. X-ray absorption spectra (XAS) were collected between 6.9 and 7.9 keV at station A-3 of the Cornell High Energy Synchrotron Source (CHESS) and at beamline X9A of the National Synchrotron Light Source (NSLS) at Brookhaven National Laboratories. The monochromator was calibrated by using the 7113.0-eV 1s → 3d peak in the XAS spectrum of $[Et_4N][FeCl_4]$ (suspended in Duco cement). The XAS data were obtained at 100 K. A_{exp} (C_f/C_0) was determined from an incident (C_0) ionization detector and a final fluorescence (C_f) detector. A large solid-angle Lytle fluorescence detector was used with a Mn filter and Soller slits (Stern & Heald, 1979).

The treatment of the raw EXAFS data to yield χ is discussed at length in several review articles (Teo, 1981; Scott, 1985). A modification of the program EXAPLT was employed to extract χ from A_{exp} by using a three-region cubic spline function. Iron–ligand distances were determined by least-squares refinement using the Newton–Gauss algorithm and locally developed software. The refinements reported were on $k^3\chi$ data, and the function minimized was $R \equiv [\sum k^6(\chi_c - \chi)^2/n]^{1/2}$, where the sum is over n data points between 2 and 14 Å^{-1} (Scarrow et al., 1987).

Use of Theoretical Phase and Amplitude Functions. Single-scattering EXAFS theory allows each shell of n scatterers at a distance $r \pm \sigma$ to be modeled separately, with the EXAFS spectrum described as a sum of each shell (Scarrow et al., 1987)

$$\chi_c = \sum_{\text{shells}} nA[f(k)k^{-1}r^{-2}e^{-2\sigma^2k^2} \sin [2kr + \alpha(k)]] \quad (1)$$

where $k = [8\pi^2m_e(E - 7125 \text{ eV} + \Delta E)/h^2]^{1/2}$. The amplitude reduction factor (A) and the shell-specific edge shift (ΔE) are empirical parameters that partially compensate for imperfections in the theoretical amplitude and phase functions f and α (Teo & Lee, 1979).

Our analysis procedure, a variation of FABM (fine adjustment based on models) (Teo et al., 1983), uses theoretical amplitude and phase functions. For each shell, known crystal structures are used to determine A, ΔE, and, for Fe–C interactions, where n would be unknown in the protein structures, σ^2 (Teo & Lee, 1979). This leaves two parameters per shell (r and σ^2 or n) to be refined instead of the four parameters refined using BFBT ("best fit based on theory") (Teo et al., 1983).

Recent studies have indicated that the single-scattering EXAFS theory is valid to lower energies than previously believed (Bunker & Stern, 1984; Müller & Schaich, 1983). However, the amplitude and phase function tables of Teo and Lee (1979) were calculated by using a plane wave approximation for the scattering of the photoelectron wave by the neighboring atom and are unsatisfactory at low photoelectron momentum. Recently McKale et al. (1988) have calculated amplitude and phase shift functions for $2 \leq k \leq 20$ Å^{-1} using a curved-wave formalism, thus extending the range of EXAFS data that can be used in refinement to $k = 2$ Å^{-1}. Use of these "curved-wave" functions have consistently yielded better fits than those determined with the Teo–Lee tables. Using the data at low photoelectron momentum raises the question as to whether other effects such as XANES may be contributing to the EXAFS spectrum. However, in both model compounds and proteins, analysis of the data in the range $2 \leq k \leq 14$ gave identical fits as when the data between $3 \leq k \leq 14$ or even $4 \leq k \leq 14$ was used. Thus, it can be assumed that contributions from phenomena other than EXAFS are negligible in the k range ($2 \leq k \leq 14$) utilized in the fits presented here.

Integration of the 1s → 3d Peak. The preedge peak areas were calculated by subtracting an arctangent function from the data and normalizing with respect to the edge jump height. The background function was determined by a least-squares fit of an arctangent together with a first-order polynomial to the data below the inflection point to the edge as previously described (Roe et al., 1984). The area of the preedge peak after the background subtraction was obtained by integrating over a range of 8 eV. This range centered on the peak and any residual background function was interpolated over that range. The edge jump was determined by fitting first-order polynomials to the data as previously described (Roe et al, 1984). The difference between these two lines at the inflection point of the edge was used as the normalization factor for the preedge peak area. For example, the native 3,4-PCD from *B. fuscum* has a normalized preedge peak area of 12.9 × 10^{-2} eV, which is abbreviated as 12.9 units.

Results and Discussion

Native 3,4-PCD. The position of the Fe K-absorption edge of 3,4 PCD from *B. fuscum* is consistent with the iron being in a ferric oxidation state. The XANES spectrum of the Fe K-edge region shows a definite absorption band about 10 eV below the midpoint of the absorption edge that can be assigned to the iron 1s → 3d transition (Figure 1A) (Shulman et al., 1976). Previous EXAFS studies on model compounds and molecular orbital calculations have demonstrated that the intensity of this preedge feature relative to the edge jump height can be correlated with the amount of iron 4p and 3d orbital mixing and, consequently, with the ligand geometry around the iron atom (Roe et al., 1984). In general, the amount of 4p and 3d orbital mixing, and therefore the peak

Table I: Results from Restricted Fits of First-Coordination-Sphere Fourier-Filtered EXAFS Spectra of 3,4-PCD

		first shell			second shell			third shell				
	fit no.	O	R (Å)	σ^2	N	R (Å)	σ^2	O	R (Å)	σ^2	F^a	Figure
3,4-PCD	1	5	1.94	0.012							0.516	
	2	3	1.90	0.0050	2	2.08	0.0060				0.127	3
	3	2	1.87	0.0027	3	2.04	0.0090				0.121	
3,4-PCD + terephthalate	4	3	1.93	0.0047	2	2.13	0.0044				0.231	4A
	5	3	1.94	0.0050	2	2.15	0.0044	1	2.46	0.0023	0.131	4B
	6	2	1.92	0.0043	4	2.09	0.014	1	2.46	0.0008	0.098	
	7	4	1.95	0.0076	2	2.18	0.0049	1	2.45	0.0013	0.084	4C
3,4-PCD + HPCA	8	5	1.99	0.0035							0.130	5
	9	4	1.97	0.0029	1	2.22	0.0029				0.144	
	10	3	1.97	0.0014	2	2.10	0.025				0.111	
	11	3	1.97	0.0012	2	2.16	0.004				0.400	

[a] F, the goodness of fit, is defined as rms(dev)/rms(dat) where the function minimized is $R \equiv [\sum k^6(\chi_c - \chi)^2/n]^{1/2}$ as described in the text.

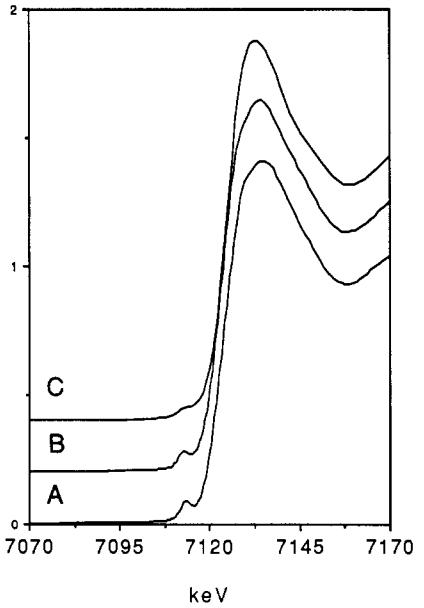

FIGURE 1: XANES data of (A) native 3,4-PCD, (B) 3,4-PCD + HPCA, and (C) 3,4-PCD + terephthalate. The areas of the preedge transitions are 12.9, 13.0, and 6.9 units, respectively. The intensity of the 1s → 3d preedge peak indicates that the ferric site remains pentacoordinate upon the binding of HPCA but becomes six coordinate upon the addition of terephthalate.

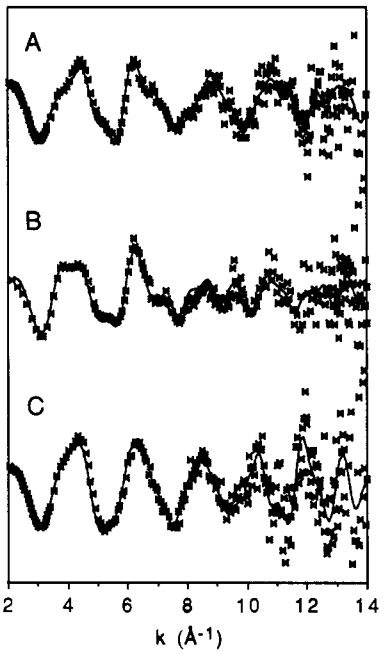

FIGURE 2: Raw (*) and Fourier-filtered (—) (back transform 1.0–5.0 Å) $k^3\chi$ data of (A) native 3,4-PCD, (B) 3,4-PCD + terephthalate, and (C) 3,4-PCD + HPCA.

intensity, increases with a reduction of the coordination number, i.e., $I_{\text{tetrahedral}} > I_{\text{5-coordinate}} > I_{\text{octahedral}}$. The area of the preedge feature of 3,4-PCD from *B. fuscum* is 12.9 units and is within the range of intensities for a 5-coordinate species. The intensity of the 1s → 3d absorption band together with the presence of a crystallographically determined 5-coordinate iron site in the 3,4-PCD from *P. aeruginosa* (Ohlendorf et al., 1988) strongly implies that the 3,4-PCD from *B. fuscum* is likewise 5-coordinate.

The unfiltered and filtered $k^3\chi$ data for 3,4-PCD is shown in Figure 2. The quality of the data is limited by the necessity of a dilute protein sample. The consequent noise is in part compensated by the large number of data points measured and does not become prohibitive until $k > 13$ Å^{-1}. Fourier filtering can be used to study contributions to the EXAFS spectrum arising from the first coordination sphere of the iron. The Fourier-filtered (back transform 1.1–2.3 Å) EXAFS spectrum of the first coordination sphere of 3,4-PCD from *B. fuscum* is shown in Figure 3. A one-shell fit (fit 1 in Table I) affords an average metal–ligand distance of 1.94 Å; however, the large Debye–Waller factor suggests the need for a second shell to model the first coordination sphere. The addition of a second shell in the simulations dramatically improves the goodness of fit, which justifies its inclusion. The data can be simulated

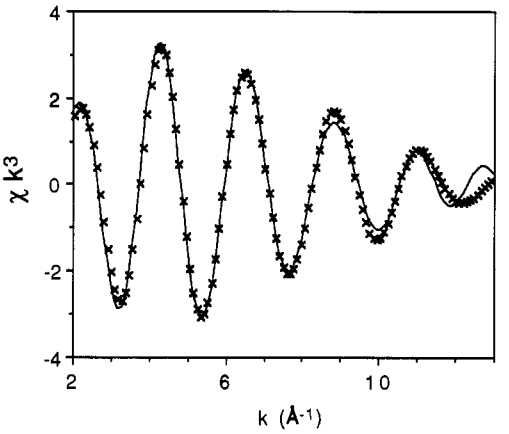

FIGURE 3: Two-shell restricted fits (—) to Fourier-filtered (back transform 1.1–2.3 Å) $k^3\chi$ EXAFS data (×) of protocatechuate 3,4-dioxygenase. The data were modeled by using 3 O/N scatterers at 1.90 Å and 2 O/N scatterers at 2.08 Å. The other parameters are as listed in Table I (simulation 2).

with comparable goodness of fit using 3 O/N atoms at 1.90 Å and 2 O/N atoms at 2.08 Å (fit 2 in Table I) or using 2 O/N atoms at 1.87 Å and 3 O/N atoms at 2.04 Å (fit 3 in Table I). However, we favor fit 2 upon consideration of the established protein ligands for 3,4-PCD and the unreasonably

large Debye–Waller factor associated with the second shell in fit 3.

Though oxygen and nitrogen ligation cannot be unequivocally distinguished by EXAFS spectroscopy, the different shells can be assigned to the crystallographically determined active site ligands by comparisons with suitable model complexes. In non-heme high-spin ferric complexes, Fe(III)–$O_{phenolate}$ bond lengths have a range of 1.87–1.95 Å (Magurany & Strouse, 1982; Davis et al., 1986; Heistand et al., 1982a; Lauffer et al., 1983), while Fe(III)–N bond lengths for imidazole (or pyrazole) range from 2.10 to 2.24 Å for high-spin model compounds (Armstrong & Lippard, 1984; Davis et al., 1986; Gomez-Romero et al., 1988; Armstrong et al., 1984; Chen et al., 1988).

In fit 2, the 1.90-Å distance can be ascribed to tyrosine ligation, while the 2.08-Å distance is consistent with histidine coordination. The Fe–$O_{solvent}$ bond is then ascribed a length of ca. 1.90 Å. Such a short distance is best associated with a coordinated hydroxide. Fe(III)–OH_2 bond lengths average ~2.06 Å (Hamor et al., 1964; Ou et al., 1978; Murphy et al., 1982; Murch et al., 1987), although they may be as short as 2.01 Å, as in $[Fe_2(5\text{-Me-HXTA})(OH)(H_2O)_2]$[1] (Murch et al., 1987), or as long as 2.15 Å, as in $[Fe(PIH)Cl_2(H_2O)]$ (Murphy et al., 1982). Fe(III)–OH bonds are expected to be shorter than Fe(III)–OH_2 bonds. The only crystallographically characterized ferric compound with a terminal hydroxide ligand, [α,γ-di-*tert*-butyloctaethyl-α,γ-dihydroporphinato]-hydroxoiron(III), has an Fe(III)–OH bond distance of 1.886 Å (Buchler et al., 1982). Most of the structural data on Fe–OH compounds are for (μ-hydroxo)diiron species, which would be expected to exhibit somewhat longer Fe–O bond lengths, e.g., 1.94 Å for $[Fe_2(5\text{-Me-HXTA})(OH)(H_2O)_2]$ (Murch et al., 1987), 1.96 Å for $[Fe_2(OH)\{HB(pz)_3\}_2(OAc)_2]ClO_4$ (Armstrong & Lippard, 1984), and 2.02 Å for $[(TACN)_4Fe_4(\mu\text{-}O)_2(\mu\text{-}OH)_4]I_4$ (Drüeke et al., 1989).

In fit 3, we would similarly ascribe tyrosine and histidine ligation to the first and second shells, respectively, on the basis of the bond length differences. The Fe–$O_{solvent}$ bond would then be ca. 2.04 Å long, which is more consistent with a coordinated water. However the Fe–N_{His} bonds would be much too short at 2.04 Å, given the weight of the model data. One way to rationalize this low value with histidine ligation would be to include a shorter bond in the second shell at 1.96 Å. The average of two Fe–N_{His} bonds at 2.08 Å and one Fe–$O_{solvent}$ bond at 1.96 Å would give the fit value of 2.04 Å, and the range spanned by these bonds would explain the large Debye–Waller factor. A solvent distance of 1.96 Å would again indicate a coordinated hydroxide.

Two other observations support the presence of a hydroxide ligand. First, the Lewis acidity of a 5-coordinate ferric ion with two neutral nitrogen ligands is expected to be large enough to lower the pK_a of a coordinated water molecule and result in its deprotonation at neutral pH; note, for example, the ready formation of oxo-bridged complexes of bis(salicylidenamine)iron(III) (Mukherjee et al., 1988; Murray, 1974). Second, NMR water relaxation studies on 3,4-PCD from *P. aeruginosa* are consistent with the presence of a single proton 2.7 Å from the iron center (Felton et al., 1984), which is at the appropriate distance for the proton on a coordinated hydroxide. Taken together, these observations suggest that the coordinated solvent in 3,4-PCD is a coordinated hydroxide rather than water.

Though the amino acid sequence of the enzyme from *B. fuscum* is not known, the residues that are ligated to the iron in the 3,4-PCD from *P. aeruginosa* are conserved in the other intradiol dioxygenases that have been sequenced (Kohlmiller & Howard, 1979a,b, Iwaki, et al., 1981; Franz & Chakrabarty, 1987; Neidle et al., 1988; Zylstra et al., 1989; Hartnett et al., 1990). Furthermore, the intensity of the preedge feature in the XANES region is similar in the two species (Roe et al., 1984). The EXAFS data indicate that the ligation of the Fe is similar, and in all likelihood identical, in the two isofunctional 3,4-PCD enzymes. These results indicate that the active site of 3,4-PCD should be revised as shown:

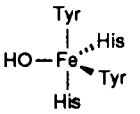

3,4-PCD + Terephthalate. Terephthalate is a competitive inhibitor of 3,4-PCD, suggesting that it occupies the same binding site as the substrate (Whittaker & Lipscomb, 1984). Since substrates are known to bind directly to the iron, similar coordination of the carboxylate moiety of terephthalate is likely. Spectroscopic changes observed for 3,4-PCD upon terephthalate binding are consistent with the coordination of the carboxylate. The 3,4-PCD–terephthalate complex exhibits an EPR spectrum markedly different from that of the uncomplexed enzyme, and the zero-field splitting parameter D changes from positive to negative on formation of the complex, indicating that the iron environment is significantly perturbed (Whittaker & Lipscomb, 1984). In addition, the hyperfine broadening found in the EPR spectrum of native 3,4-PCD in $^{17}OH_2$ is not observed for the terephthalate complex with the enzyme prepared in $^{17}OH_2$-enriched buffer solutions (Whittaker & Lipscomb, 1984), suggesting that the iron–solvent interaction has been eliminated or significantly weakened.

The tyrosine-to-metal charge-transfer band in the optical spectrum of the enzyme-terephthalate complex is red shifted relative to that of the uncomplexed enzyme. Previous model studies on Fe(salen)X complexes have demonstrated that the more basic the ligand coordinated to the iron the more blue shifted the salen-to-iron(III) charge-transfer band (Pyrz et al., 1985). These studies are also applicable to the tyrosinate-to-Fe(III) charge-transfer bands in 3,4-PCD's and catechol 1,2-dioxygenases (Heistand et al., 1982b). The red shift seen upon addition of terephthalate to 3,4-PCD indicates an increase in the Lewis acidity of the active site ferric center, consistent with replacement of the coordinated hydroxide with the less basic carboxylate.

The XANES spectrum of the enzyme–terephthalate complex suggests a change in the iron coordination environment relative to that of the native enzyme. The preedge feature is dramatically less intense than is found for the native enzyme (Figure 1C) with a peak area of 6.9 units. This suggests that the ligation of terephthalate diminishes the 3d–4p orbital mixing in the iron and makes the iron environment more centrosymmetric. We thus propose that the iron becomes 6-coordinate in the 3,4-PCD–terephthalate complex. This change in environment could occur following one of several binding scenarios including monodentate or bidentate coordination of the terephthalate carboxylate moiety coupled with retention or elimination of the coordinated solvent. However,

[1] Abbreviations: acac, acetylacetonate; $catH_2$, catechol; cyclen, 1,4,7,10-tetraazacyclododecane; EDTA, ethylenediaminetetraacetate; $HB(3,5\text{-}iPr_2p)_3$, hydrotris(3,5-diisopropyl-1-pyrazolyl)borate; HPCA, homoprotocatechuate; hq, hydroquinone; 5-Me-HXTA, *N,N'*-(2-hydroxy-5-methyl-1,3-xylylene)bis[*N*-(carboxymethyl)glycine]; OAc, acetate; OBz, benzoate; PCA, protocatechuate; 3,4-PCD, protocatechuate 3,4-dioxygenase; PIH, pyridoxal isonicotinoyl hydrazone; salen, ethylenebis(salicylidenamine); PSQ, phenanthrene semiquinone; saloph, *o*-phenylenebis(salicylidenamine).

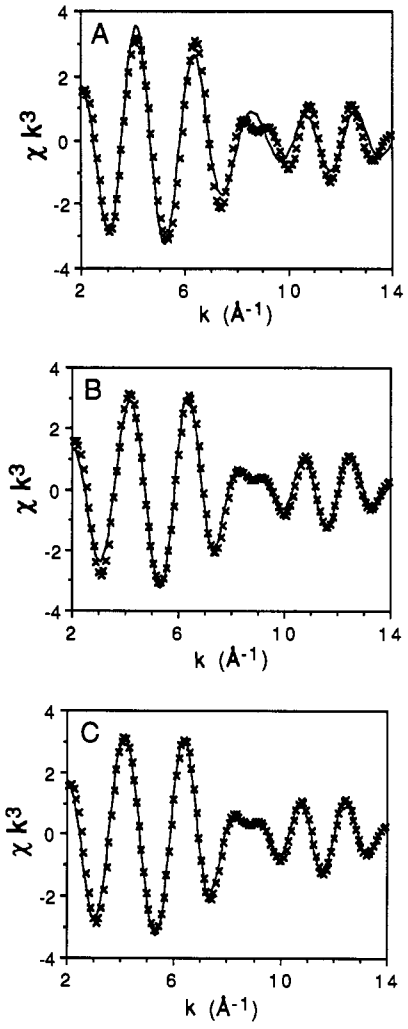

FIGURE 4: Two- (A) and three-shell (B) and (C) restricted fits (—) to Fourier-filtered (back transform 1.1–2.4 Å) $k^3\chi$ EXAFS data (×) of the 3,4-PCD–terephthalate complex. Parameters are as listed in Table I (simulations 4, 5, and 7, respectively).

another scenario in which the iron becomes 6-coordinate by addition of a new ligand from the protein in addition to a monodentate terephthalate is unlikely because the X-ray structure shows no other potential ligands near the iron (Ohlendorf et al., 1988).

The Fourier-filtered EXAFS spectrum (back transform 1.1–2.4 Å) of 3,4-PCD complexed with terephthalate (Figure 4) shows a definite beat pattern, i.e., a perturbation of the oscillations at $k \sim 9$ Å^{-1}; this beat pattern is also discernible in the unfiltered data (Figure 2). An attempt was made to simulate the observed spectrum under the assumption that the solvent molecule is displaced by terephthalate and the iron remains 5-coordinate. Figure 4A shows a fit to the spectrum assuming 3 Fe–O bonds at 1.93 Å and 2 Fe–N bonds at 2.13 Å (fit 4). Although satisfactory at low k values, this fit matches the data poorly at higher k values and fails to reproduce the beat pattern. This pattern could not be duplicated without the presence of a low Z scatterer at 2.46 Å (fit 5 in Table I; Figure 4B) in addition to the first two shells.[2] Two other parameter sets which give simulations that match the experimental data well (fits 6 and 7 in Table I; Figure 4C) also require the 2.46-Å shell. However, fit 6 has an unreasonably large Debye–Waller factor in the second shell and will not be considered further.

In the fits for the terephthalate complex, the Fe–O_{Tyr} and Fe–N_{His} bond lengths increase relative to those of the native enzyme, as expected for an increase in coordination number. These increased bond lengths are precedented by the Fe(III)–salen complexes (Gerloch & Mabbs, 1967; Heistand et al., 1982a; Lauffer et al., 1983). For example, the 5-coordinate complexes $[Fe(salen)]_2hq$ and [Fe(salen)Cl] have Fe–O distances of 1.91 and 1.88 Å and Fe–N distances of 2.10 and 2.08 Å, respectively, while the 6-coordinate [Fe(salen)(acac)] and [Fe(salen)PSQ] have slightly longer Fe–O (1.93 and 1.92 Å, respectively) and Fe–N (2.12 and 2.14 Å, respectively) bond lengths. However, an added factor to the increase in the average Fe–O bond length of the 3,4-PCD–terephthalate complex is also the replacement of the Fe–hydroxide bond with a longer Fe–carboxylate bond (Buchler et al., 1982; Carrell et al., 1988), which on the average is 2.01 Å but may range from 1.90 to 2.08 Å (Oumous et al., 1984; Vincent et al., 1988).

We ascribe the 2.46-Å scatterer to a feature of terephthalate carboxylate coordination; reasonable candidates for this scatterer are the carbon of a symmetrically chelated carboxylate or the more distant oxygen of an asymmetrically chelated carboxylate. A symmetrically chelated carboxylate mode would result in a four-membered ring for which the stability apparently depends on maintaining the carboxylate O–C–O angle at ~120° and keeping the O–M–O angle reasonably large (>60°) (Carrell et al., 1988). Such considerations would require an average Fe–$O_{carboxylate}$ distance of 2.15 Å to afford an Fe–C distance of 2.46 Å.[3] The assignment of the chelated carboxylate oxygens to the second shell in fits 5 and 7 would require Fe–N_{His} bonds to be included in the first shell, but such distances are much too short for imidazole ligation. Thus neither fit supports a symmetrically chelated carboxylate in the 3,4-PCD active site.

Asymmetric carboxylate binding is more readily rationalized in the context of the data simulations. Fit 5 in Table I has three Fe–O/N interactions at 1.94 Å and 2 Fe–O/N interactions at 2.15 Å in addition to the scatterer at 2.46 Å. In this model, one carboxylate oxygen is placed at 1.94 Å while the second, more weakly coordinated oxygen is placed at 2.46 Å, representing the low Z scattering atom,[4] i.e.

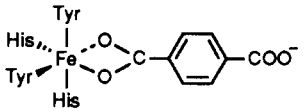

The iron coordination environment associated with fit 7 would be similar to that shown above but would be modified by the retention of a solvent molecule to afford a 7-coordinate complex. The four atoms in the first shell would consist of the two tyrosine oxygens, a carboxylate oxygen, and a solvent oxygen. The coordination number of 7 would still be consistent with the area of the preedge feature, since the 7-coordinate $Na[Fe(EDTA)H_2O]$ also exhibits a preedge feature whose area is in the range found for 6-coordinate complexes (Roe et al., 1984). However, the absence of any hyperfine broad-

[2] We have examined several 5-coordinate and 6-coordinate iron model complexes which have one long Fe–O/N bond of ~2.4 with EXAFS spectroscopy. In all cases, a shell corresponding to this scatterer was needed to simulate the Fourier-filtered first-coordination-sphere data.

[3] The distance of 2.46 Å was calculated by assuming a C–O distance of 1.3 Å and a ∠O–C–O of 120°.

[4] Using Fe–$O_{carboxylate}$ distances of 1.98 and 2.46 Å and C–O bond lengths of 1.3 Å, the carbon from the carboxylate was calculated to be at 2.6 Å. This interaction is outside the Fourier-filtering region employed in these simulations and as such would not be expected to contribute significantly to the filtered EXAFS pattern. Indeed, increasing the third shell to two atoms did not result in a good fit.

ening in the EPR signal from ^{17}O-labeled solvent in the 3,4-PCD–terephthalate complex (Whittaker & Lipscomb, 1984) is inconsistent with the retention of a coordinated solvent molecule on the basis of the accumulated EPR data on the effects of $H_2{}^{17}O$ on the spectra of various 3,4-PCD complexes (Orville & Lipscomb, 1989). We thus favor the model associated with fit 5 to describe the iron site of the of the 3,4-PCD–terephthalate complex.

The proposed asymmetric carboxylate coordination mode is precedented in two ferrous model complexes, [Fe(OBz)(MeCN)(HB(3,5-i-Pr_2pz)$_3$)] (Kitajima et al., 1990) and [Fe(cyclen)(OAc)](CF_3SO_3) (K. Hagen, personal communication); in these structures, the Fe–O distances for the carboxylate group differ by 0.11 and 0.30 Å, respectively. In the three structually characterized ferric complexes where the carboxylate is free to choose its coordination mode, the carboxylate is essentially monodentate and coordinates to the Fe^{3+} ion in the *z* configuration through the more basic syn lone pair on the carboxylate oxygen with the other carboxylate oxygen 2.9–3.1 Å away (Eremenko et al., 1983; Oumous et al., 1984; Menage & Que, 1990). In this configuration, a decrease of ∠Fe–O–C would engender the proposed asymmetric chelation mode.

3,4-PCD + HPCA. There is strong evidence indicating that substrate binds to 3,4-PCD in a bidentate manner (Lauffer & Que, 1982; Pyrz et al., 1985; Orville & Lipscomb, 1989), the most definitive being from EPR studies of the 3,4-PCD–HPCA complex (Orville & Lipscomb, 1989). The line broadening of the dominant rhombic EPR signal (g = 9.68, 4.28) seen upon selective ^{17}O labeling of either the 3-OH or the 4-OH moieties shows that the slow substrate HPCA can coordinate to the iron through both of its hydroxyl functions. Moreover, no broadening of the EPR resonances from $^{17}OH_2$ is observed for this complex, suggesting that the solvent ligand to the Fe is displaced when HPCA binds. If the catecholate binds in a bidentate manner, it would presumably displace the solvent molecule and render the ferric ion 6-coordinate in the absence of any conformational changes as shown:

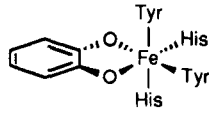

Interestingly, addition of HPCA to 3,4-PCD causes little change in the intensity of the preedge feature (13.0 units in the 3,4-PCD–HPCA complex compared to 12.9 units in the native enzyme, Figure 1), indicating that the ferric ion remains 5-coordinate in the 3,4-PCD–HPCA complex. As such, the above model must be incorrect and one of the endogenous protein ligands must be displaced. The 3,4-PCD–HPCA EXAFS data can be reasonably fit to either a single shell of 5 O/N scatterers at 1.99 Å from the ferric ion (Figure 5; fit 8 in Table I) or two shells of scatterers with 4 O/N at 1.97 Å and 1 O/N at 2.22 Å (fit 9). Fits consisting of 3 O/N at ~1.97 Å and 2 O/N at ~2.10 Å afford either an unusually large Debye–Waller factor for the scatterers at ~2.1 Å (fit 10) or a significantly poorer F value (fit 11).

On the basis of fit 8 or 9, the average Fe–O/N distance seen by EXAFS represents a significant lengthening of the Fe–O_{Tyr} bonds relative to those of the native enzyme. However, this lengthening is precedented in model systems. Fe(saloph)catH, a complex with a monodentate catechol, has Fe–$O_{catecholate}$ and Fe–$O_{phenolate}$ distances of 1.83 and 1.90 Å, respectively (Heistand et al., 1982a). In the chelated catecholate complex [Fe(salen)cat]$^-$, all four Fe–O bonds are 1.99 Å long (Lauffer et al., 1983), closely matching those found by EXAFS for the

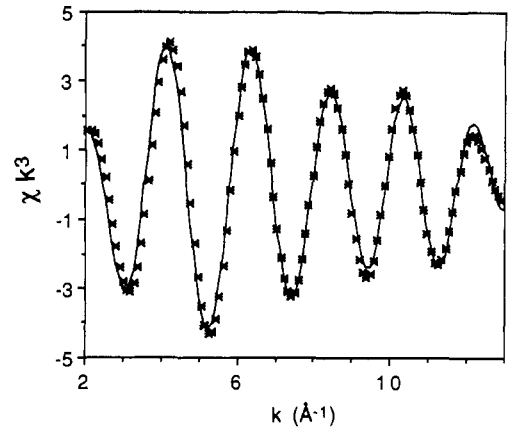

FIGURE 5: One-shell restricted fit (—) to Fourier-filtered (back transform 1.1–2.3 Å) $k^3\chi$ EXAFS data (*) of the 3,4-PCD-HPCA complex. The data were modeled with 5 O/N scatterers at 1.99 Å; the other parameters are as listed in Table I (simulation 8).

3,4-PCD–HPCA complex. The 2.22-Å distance in the 2-shell fit would then correspond to a histidine ligand, its longer distance also being a result of catechol chelation (Lauffer et al., 1983). Taken together, the X-ray absorption data suggest that the HPCA chelates to the Fe, displacing an axial ligand as well as the hydroxide ligand as shown:

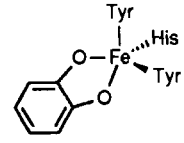

It cannot be determined whether the 3-OH or 4-OH group coordinates in the equatorial position. Likewise, the identity of the displaced axial ligand cannot be determined unequivocally. For purposes of illustration we have portrayed the histidine as being displaced upon chelation of substrate. The observed Fe–O/N distance of 1.99 Å in the 3,4-PCD–HPCA complex is more consistent with an 1N/4O coordination environment than with an 2N/3O array. Furthermore, in studies on the interaction of 3-chloro-4-hydroxybenzoate with 3,4-PCD from *P. aeruginosa*, Felton et al. (1982) have suggested that the inhibitor displaces a histidine ligand upon binding to the ferric site, because of the reduction of area of the second-shell Fe–C peak in the Fourier-transformed EXAFS data compared to that of the native enzyme and the loss of the ν(Fe–N_{His}) stretch at 274 cm^{-1} observed in the resonance Raman spectrum of the native enzyme. Unfortunately, attempts to determine the number of bound histidines from our data by analyzing the contributions of more distant atoms using multiple-scattering techniques have yielded inconclusive results due to the insufficient signal-to-noise ratios of the data.

The X-ray absorption data thus favor a 5-coordinate iron complex for the enzyme–substrate complex. Such a conclusion is also consistent with the acid–base chemistry associated with substrate binding and required by the crystal structure data. From a chemical standpoint, the displacement of an endogenous ligand from the ferric active site may be necessary for catecholate binding. Since the first pK_a's of the hydroxyl moieties of PCA and HPCA are 8.84 and 9.50, respectively, the substrate retains its full complement of catechol protons at neutral pH (Smith & Martell, 1982). The spectral changes resulting from substrate binding to the active site iron require the loss of both hydroxyl protons, presumably to nearby bases in the enzyme active site. However, the crystal structure of native 3,4-PCD from *P. aeruginosa* shows that there are no bases in the active site, save the five iron ligands (D. H. Ohlendorf and J. D. Lipscomb, unpublished data). On dis-

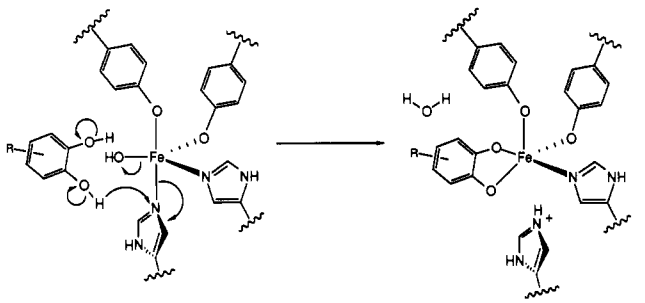

FIGURE 6: Mechanism for the chelation of substrate to protocatechuate 3,4-dioxygenase. In this proposed scheme the axial histidine is displaced when it acts as a base to deprotonate the catecholate substrate. However, it cannot be determined whether the 3-OH or the 4-OH group binds in the equatorial position, and the displacement of the axial tyrosine instead of the histidine cannot be ruled out.

placement, the coordinated OH could provide one of the protonation sites, but the second site may be provided by displacement of one of the protein ligands to the iron (Figure 6). The EXAFS fits would appear to favor the displacement of one of the His ligands since the dominant bond length obtained is more consistent with oxygen rather than nitrogen coordination. However, displacement of the axial tyrosine cannot be dismissed due to the difficulties inherent in fitting EXAFS data for a complex in which all the ligands are oxygen and nitrogen.

The putative binding cavity for the aromatic ring in substrates and inhibitors observed in the crystal structure of 3,4-PCD provides another argument for the proposed mode of binding. Extensive modeling of the crystal structure of native 3,4-PCD with van der Waals surfaces suggests that the orientation of the aromatic binding site will not allow the catecholate substrate to approach the ferric site in an orientation where both oxygens coordinate in the equatorial plane (D. H. Ohlendorf and J. D. Lipscomb, unpublished data). In the absence of major changes in the protein conformation upon the interaction with substrate, the catechol ring must be oriented nearly perpendicular to the equatorial plane. The catecholate oxygens would then occupy equatorial and axial positions, respectively, as shown in Figure 6. In the case of the terephthalate complex, the aromatic ring can bind in the same orientation as the substrate, but the carboxylate is not constrained to remain coplanar with the ring and could rotate to chelate to the iron in the equatorial plane. These results demonstrate that EXAFS spectroscopy can provide important insights into the differing interactions of substrate and inhibitor with an enzyme active site.

ACKNOWLEDGMENTS

We thank Dr. Syed Khalid of the National Biostructures PRT for his help at beamline X9A at NSLS. The PRT is supported by the National Institutes of Health (RR-01633), while CHESS is supported by the National Science Foundation (DMR-8412465).

Registry No. HPCA, 102-32-9; L-His, 71-00-1; L-Tyr, 60-18-4; 3,4-PCD, 9029-47-4; Fe, 7439-89-6; OH^-, 14280-30-9; terephthalic acid, 100-21-0.

REFERENCES

Armstrong, W. H., & Lippard S. J. (1984) *J. Am. Chem. Soc. 106*, 4632–4633.

Armstrong, W. H., Spool, A. Papaefthymiou, G. C., Frankel, R. B., & Lippard, S. J. (1984) *J. Am. Chem. Soc. 106*, 3653–3667.

Buchler, J. W., Lay, K. L., Lee, Y. J., & Scheidt, W. R. (1982) *Angew. Chem., Int. Ed. Engl. 21*, 432.

Bull, C., Ballou, D. P., & Otsuka, S. (1981) *J. Biol. Chem. 256*, 12681–12686.

Bunker, G. B., & Stern, E. A. (1984) *Phys. Rev. Lett. 52*, 1990–1993.

Carrell, C. J., Carrell, H. L., Erlebacher, J., & Glusker, J. P. (1988) *J. Am. Chem. Soc. 110*, 8651–8656.

Chen, Q., Lynch, J. B., Gomez-Romero, P., Ben-Hussein, A., Jameson, G. B., O'Connor, C. J., & Que, L., Jr. (1988) *Inorg. Chem. 27*, 2673–2681.

Cox, D. D., & Que, L., Jr. (1988) *J. Am. Chem. Soc. 110*, 8085–8092.

Davis, J. C., Kung, W. S., & Averill, B. A. (1986) *Inorg. Chem. 25*, 394–396.

Drüeke, S., Wieghardt, K., Nuber, B., Weiss, J., Bominaar, E. L., Sawaryn, A., Winkler, H., & Trautwein, A. X. (1989) *Inorg. Chem. 28*, 4477–4483.

Durham, D. R., Stirling, L. A., Ornston, L. N., & Perry, J. J. (1980) *Biochemistry 19*, 149–155.

Eremenko, I. L., Pasynskii, A. A., Orazsakhatov, B., Ellert, O. G., Novotortsev, V. M., Kalinnikov, V. T., Porai-Koshits, M. A., Antsyshkina, A. S., Dikareva, L. M., & Ostrikova, V. N. (1983) *Inorg. Chim. Acta 73*, 225–229.

Felton, R. H., Cheung, L. D., Phillips, R. S., & May, S. W. (1978) *Biochem. Biophys. Res. Commun. 85*, 844–850.

Felton, R. H., Barrow, W. L., May, S. W., Sowell, A. L., Goel, S., Bunker, G., & Stern, E. A. (1982) *J. Am. Chem. Soc. 104*, 6132–6134.

Felton, R. H., Gordon, S. L., Sowell, A. L., & May, S. W. (1984) *Biochemistry 23*, 3955–3959.

Franz, B., & Chakrabarty, A. M. (1987) *Proc. Natl. Acad. Sci. U.S.A. 84*, 4460–4464.

Fujisawa, H., & Hayaishi, O. (1968) *J. Biol. Chem. 243*, 2673–2681.

Gerloch, M., & Mabbs, F. E. (1967) *J. Chem. Soc. A*, 1598–1608.

Gomez-Romero, P., Casan-Pastor, N., Ben-Hussein, A., & Jameson, G. B. (1988) *J. Am. Chem. Soc. 110*, 1988–1990.

Hamor, M. J., Hamor, T. A., & Hoard, J. L. (1964) *Inorg. Chem. 3*, 34–43.

Hartnett, C., Neidle, E. L., Ngai, K. L., & Ornston, L. N. (1990) *J. Bacteriol. 172*, 956–966.

Heistand, R. H., II, Roe, A. L., & Que, L., Jr. (1982a) *Inorg. Chem. 21*, 676–681.

Heistand, R. H., II, Lauffer, R. B., Fikrig, E., & Que, L., Jr. (1982b) *J. Am. Chem. Soc. 104*, 2789–2796.

Iwaki, M., Kagamiyama, H., & Nozaki, M. (1981) *Arch. Biochem. Biophys. 210*, 210–223.

Keyes, W. E., Loehr, T. M., & Taylor, M. L. (1978) *Biochem. Biophys. Res. Commun. 83*, 941–945.

Kitajima, N., Fukui, H., Moro-oka, Y., Mizutani, Y., & Kitagawa, T. (1990) *J. Am. Chem. Soc. 112*, 6402–6403.

Kohlmiller, N. A., & Howard, J. B. (1979a) *J. Biol. Chem. 254*, 7302–7308.

Kohlmiller, N. A., & Howard J. B. (1979b) *J. Biol. Chem. 254*, 7309–7315.

Lauffer, R. B., & Que, L., Jr. (1982) *J. Am. Chem. Soc. 104*, 7324–7325.

Lauffer, R. B., Heistand, R. H., II, & Que, L., Jr. (1983) *Inorg. Chem. 22*, 50–55.

Magurany, C. J., & Strouse, C. E. (1982) *Inorg. Chem. 21*, 2348–2350.

McKale, A. G., Veal, B. W., Paulikas, A. P., Chan, S.-K., & Knapp, G. S. (1988) *J. Am. Chem. Soc. 110*, 3763–3768.

Menage, S., & Que, L., Jr. (1990) *Inorg. Chem. 29*, 4293–4297.

Mukherjee, R. N., Stack, T. D. P., & Holm, R. H. (1988) *J. Am. Chem. Soc. 110*, 1850–1861.
Müller, J. E., & Schaich, W. L. (1983) *Phys. Rev. B 27*, 6489–6492.
Murch, B. P., Bradley, F. C.,Boyle, P. D., Papaefthymiou, V., & Que, L., Jr. (1987) *J. Am. Chem. Soc. 109*, 7993–8003.
Murphy, T. B., Johnson, D. K., Rose, N. J., Aruffo, A., & Schomaker, V. (1982) *Inorg. Chim. Acta 66*, L67–68.
Murray, K. S. (1974) *Coord. Chem. Rev. 12*, 1–35.
Neidle, E. L., Hartnet, C., Bonitz, S., & Ornston, L. N. (1988) *J. Bacteriol. 170*, 4874–4878.
Ohlendorf, D. H., Lipscomb, J. D., & Weber, P. C. (1988) *Nature 336*, 403–405.
Orville, A. M., & Lipscomb, J. D. (1989) *J. Biol. Chem. 264*, 8791–8801.
Ou, C. C., Wollman, R. G., Hendrickson, D. N., Potenza, J. A., & Schugar, H. J. (1978) *J. Am. Chem. Soc. 100*, 4717–4724.
Oumous, H., Lecomte, C., Protas, J., Cocolios, P., & Guillard, R. (1984) *Polyhedron 3*, 651–659.
Pyrz, J. W., Roe, A. L., Stern, L. J., & Que, L., Jr. (1985) *J. Am. Chem. Soc. 107*, 614–620.
Que, L., Jr. (1983) *Coord. Chem. Rev. 50*, 73–108.
Que, L., Jr. (1989) in *Iron Carriers and Iron Proteins* (Loehr, T. M., Ed.) pp 467–524, VCH, New York.
Que, L., Jr., & Epstein, R. M. (1981) *Biochemistry 20*, 2545–2549.
Que, L., Jr., Lipscomb, J. D., Zimmermann, R., Münck, E., Orme-Johnson, N. R., & Orme-Johnson, W. H. (1976) *Biochim. Biophys. Acta 452*, 320–334.
Que, L., Jr., Lipscomb, J. D., Münck, E., & Wood, J. M. (1977) *Biochim. Biophys. Acta 485*, 60–74.
Roe, A. L., Schneider, D. J., Mayer, R. J., Pyrz, J. W., Widom, J., & Que, L., Jr. (1984) *J. Am. Chem. Soc. 106*, 1676–1681.
Scarrow, R. C., Maroney, M. J., Palmer, S. M., Que, L., Jr., Roe, A. L., Salowe, S. P., & Stubbe, J. A. (1987) *J. Am. Chem. Soc. 109*, 7857–7864.
Scott, R. A. (1985) *Methods Enzymol. 11*, 414–459.
Sheriff, S., Hendrickson, W. A., & Smith, J. L. (1987) *J. Mol. Biol. 197*, 273–296.
Shulman, R. G., Yafet, Y., Eisenberger, P., & Blumberg, W. E. (1976) *Proc. Natl. Acad. Sci. U.S.A. 73*, 1384–1388.
Smith, R. M., & Martell, A. E. (1982) *Critical Stability Constants*, Vol. 5, Plenum Press, New York.
Stenkamp, R. E., Sieker, L. C., & Jensen, L. H. (1984) *J. Am. Chem. Soc. 106*, 618–622.
Stern, E. A., & Heald, S. M. (1979) *Rev. Sci. Instrum. 50*, 1579–1582.
Teo, B.-K. (1981) in *EXAFS Spectroscopy, Techniques and Applications* (Teo, B.-K., & Joy, D. C., Eds.) pp 13–58, Plenum, New York.
Teo, B.-K., & Lee, P. A. (1979) *J. Am. Chem. Soc. 101*, 2815–2832.
Teo, B. K., Antonio, M. R., & Averill, B. A. (1983) *J. Am. Chem. Soc. 105*, 3751–3762.
Vincent, J. B., Huffman, J. C., Christou, G., Li, Q., Nanny, M. A., Hendrickson, D. N., Fong, R. H., & Fish, R. H. (1988) *J. Am. Chem. Soc. 110*, 6898–6900.
Walsh, T. A., Ballou, D. P., Mayer, R., & Que, L., Jr. (1983) *J. Biol. Chem. 258*, 14422–14427.
Whittaker, J. W., & Lipscomb, J. D. (1984) *J. Biol. Chem. 259*, 4487–4495.
Whittaker, J. W., Lipscomb, J. D., Kent, T. A., & Münck, E. (1984) *J. Biol. Chem. 259*, 4466–4475.
Whittaker, J. W., Orville, A. M., & Lipscomb, J. D. (1990) *Methods Enzymol. 188*, 82–88.
Zylstra, G. J., Olsen, R. H., & Ballou, D. P. (1989) *J. Bacteriol. 171*, 5915–5921.